

***S*-, *P*- and *D*-wave $\pi\pi$ final state interactions and *CP* violation in $B^\pm \rightarrow \pi^\pm \pi^\mp \pi^\pm$ decays**

J.-P. DEDONDER AND B. LOISEAU

Laboratoire de Physique Nucléaire et de Hautes Énergies, Groupe Théorie,
Université Pierre et Marie Curie et Université Paris-Diderot, IN2P3 & CNRS,
4 place Jussieu, 75252 Paris, France

AND

A. FURMAN

ul. Bronowicka 85/26, 30-091 Kraków, Poland

AND

R. KAMIŃSKI AND L. LEŚNIAK

Division of Theoretical Physics, The Henryk Niewodniczański Institute of Nuclear
Physics, Polish Academy of Sciences, 31-342 Kraków, Poland

We study *CP* violation and the contribution of the strong pion-pion interactions in the three-body $B^\pm \rightarrow \pi^\pm \pi^\mp \pi^\pm$ decays within a quasi two-body QCD factorization approach. The short distance interaction amplitude is calculated in the next-to-leading order in the strong coupling constant with vertex and penguin corrections. The meson-meson final state interactions are described by pion non-strange scalar and vector form factors for the *S* and *P* waves and by a relativistic Breit-Wigner formula for the *D* wave. The pion scalar form factor is calculated from a unitary relativistic coupled-channel model including $\pi\pi$, $K\bar{K}$ and effective $(2\pi)(2\pi)$ interactions. The pion vector form factor results from a Belle Collaboration analysis of $\tau^- \rightarrow \pi^- \pi^0 \nu_\tau$ data. The recent $B^\pm \rightarrow \pi^\pm \pi^\mp \pi^\pm$ BABAR Collaboration data are fitted with our model using only three parameters for the *S* wave, one for the *P* wave and one for the *D* wave. We find not only a sizable contribution of the *S* wave just above the $\pi\pi$ threshold but also under the $\rho(770)$ peak a significant interference, mainly between the *S* and *P* waves. For the *B* to $f_2(1270)$ transition form factor, we predict $F^{Bf_2}(m_\pi^2) = 0.098 \pm 0.007$. Our model yields a unified unitary description of the contribution of the three scalar resonances $f_0(600)$, $f_0(980)$ and $f_0(1400)$ in terms of the pion non-strange scalar form factor.

1. Introduction

Three-body charmless hadronic B meson decays offer one of the best tools for studies of direct CP violation and provide an interesting testing ground for strong interaction dynamical models. The present work, part of a program devoted to the understanding of rare three-body B decays [1, 2, 3, 4], is motivated by the recent BABAR Dalitz-plot analysis of the $B^\pm \rightarrow \pi^\pm \pi^\mp \pi^\pm$ decays [5]. In an isobar model description, the authors of Ref. [5] find evidence for the $f_0(1370)$ but, within the current experimental accuracy, no significant signal for the $f_0(980)$. The $f_0(600)$, not explicitly included in that analysis, could be part of the non-resonant background. Furthermore, there is a small but visible contribution of the $f_2(1270)$ resonance [5].

Here, the aim is to provide a phenomenological analysis of the $B^\pm \rightarrow \pi^\pm \pi^\mp \pi^\pm$ decay channels relying on the QCD factorization scheme (QCDF) in the $\pi\pi$ effective mass range from threshold to 1.64 GeV. The focus will be set on the final state $\pi\pi$ interactions involved since a partial wave analysis of the Dalitz plot should use theoretically and phenomenologically well constrained $\pi\pi$ amplitudes.

Studies of B decays into two-body and quasi-two-body final states have been performed in the QCDF framework [6, 7, 8, 9, 10, 11, 12]. The naive factorization approach is a useful first order approximation which receives corrections proportional to the strong coupling constant α_s at scales m_b and $\sqrt{\Lambda_{QCD} m_b}$ and in inverse powers of the b quark mass m_b [13]. In the present study, we propose an extension of these results to the three-body decays $B^\pm \rightarrow \pi^\pm \pi^+ \pi^-$.

The role of the $f_0(600)$ (or σ) in charmless three-body decays of B mesons has been examined by Gardner and Meißner [8] in $B^0 \rightarrow \pi^+ \pi^- \pi^0$ decays. Within QCD quasi two-body factorization approach their $f_0(600)\pi$ amplitude is described by a unitary pion scalar form factor constrained by $\pi\pi$ scattering and chiral dynamics. This is different from the relativistic Breit-Wigner parametrization used in most experimental analyses and in some theoretical studies, for example in [14]. This has led to improved theoretical predictions; the contribution of the $f_0(600)\pi$ channel has been found to be important in the range of the dominant $\rho^0 \pi^0$ intermediate state. However, in recent $B^0 \rightarrow \pi^+ \pi^- \pi^0$ Dalitz plot analyses [15, 16] no contribution from $B^0 \rightarrow f_0(600)\pi^0$ channel has been found. This could be linked to the present limited statistics in the low effective $\pi\pi$ mass region. Furthermore, such a contribution could be hidden in the nonresonant amplitude introduced in the experimental analysis. Nevertheless we will show that the contribution of the S wave is important in the $B^\pm \rightarrow \pi^\pm \pi^+ \pi^-$ decays.

Charmless three-body decays of B mesons have also been investigated by Cheng, Chua and Soni [12] in the framework of quasi two-body factorization approach using resonant and non-resonant contributions. In particular they have calculated the $B^- \rightarrow \pi^+\pi^-\pi^-$ branching fractions and CP asymmetries and found a small rate for $B^- \rightarrow f_0(980)\pi^-$ decay.

An achievement in the theory of B decays into two mesons is the confirmation of the validity of factorization as a leading order approximation. No proof of factorization has yet been given for the B decays into three mesons. However, three-body interactions are suppressed when specific kinematical configurations with the three mesons quasi aligned in the rest frame of the B meson are considered. This is the case in the effective $\pi^+\pi^-$ mass region smaller than 1.64 GeV in the Dalitz plot where most of the $\pi^+\pi^-$ resonant states are visible. Such processes will be denoted as $B^\pm \rightarrow \pi^\pm[\pi^+\pi^-]$, the mesons of the $[\pi^+\pi^-]$ pair moving more or less, in the same direction in the B rest frame. Then, it seems reasonable to postulate the validity of factorization for this quasi two-body B decay [17] assuming that the $[\pi^+\pi^-]$ pair originates from a quark-antiquark state.

In the factorization approach the $B^\pm \rightarrow \pi_1^\pm [\pi_2^+\pi_3^-]$ decay amplitudes are expressed as a superposition of appropriate effective QCD coefficients and two products of two transition matrix elements. The transition matrix elements between the B^\pm meson and the π_1^\pm pion multiplied by the transition matrix elements between the vacuum and the $[\pi_2^+\pi_3^-]$ pion pair correspond to the first of these products. Here, in the $\pi_2^+\pi_3^-$ center of mass frame, the bilinear quark currents involved force the $[\pi_2^+\pi_3^-]$ pair to be in S or in P state. The second term is associated to the product of the transition matrix elements between the B^\pm meson and the $[\pi_2^+\pi_3^-]$ pion pair in S , P or D state by the transition matrix elements between the vacuum and the π_1^\pm pion. The $[\pi_2^+\pi_3^-]_{S,P}$ transition matrix elements to the vacuum are proportional to the pion scalar and vector form factors. We assume that the $B^\pm \rightarrow \pi_2^+\pi_3^-$ matrix elements are expressed as products of the $B^\pm \rightarrow [\pi_2^+\pi_3^-]_{S,P,D}$ transition form factors by the relevant vertex function describing the decay of the $[\pi_2^+\pi_3^-]_{S,P,D}$ state into the final pion pair. The vertex functions are in turn assumed to be proportional to the pion scalar form factor for the S wave, to the vector form factor for the P wave and to a relativistic Breit-Wigner formula for the D wave. Here, a single unitary function, namely the pion non-strange scalar form factor, describes then the three scalar resonances, $f_0(600)$, $f_0(980)$ and $f_0(1400)$ present in the $\pi^+\pi^-$ interaction.

In Sec. 2 we present the model used in the analysis. Sec. 3 is devoted to the construction of the pion scalar and vector form factors. The pertinent observables and the fitting procedure are described in Sec. 4 while the results are discussed in Sec. 5. A summary and some perspectives are outlined in

the final Sec. 6. The detailed derivation of the decay amplitudes is presented in the Appendix A while Appendix B gives the system of equations to be solved to obtain the parameters fixing the low-energy behavior of the pion scalar form factor to be that of one loop calculation in chiral perturbation theory.

2. Decay amplitudes

The amplitudes for the non-leptonic decays of the B meson are given as matrix elements of the effective weak Hamiltonian [6, 7]

$$H_{eff} = \frac{G_F}{\sqrt{2}} \sum_{p=u,c} \lambda_p \left[C_1 O_1^p + C_2 O_2^p + \sum_{i=3}^{10} C_i O_i + C_{7\gamma} O_{7\gamma} + C_{8g} O_{8g} \right] + h.c., \quad (1)$$

where

$$\lambda_u = V_{ub} V_{ud}^*, \quad \lambda_c = V_{cb} V_{cd}^*, \quad (2)$$

the $V_{pp'}$ ($p' = b, d$) being Cabibbo-Kobayashi-Maskawa quark-mixing matrix elements. For the Fermi coupling constant G_F we take the value $1.16637 \times 10^{-5} \text{ GeV}^{-2}$. The $C_i(\mu)$ are the Wilson coefficients of the four-quark operators $O_i(\mu)$ at a renormalization scale μ . The $O_{1,2}^p$ are left-handed current-current operators arising from W -boson exchange, $O_{i=3-10}$ are QCD and electroweak penguin operators involving a loop with a u or c quark and a W boson, $O_{7\gamma}$ and O_{8g} are the electromagnetic and chromomagnetic dipole operators [7].

Let p_B be the four-momentum of the B^\pm meson and p_1 that of the isolated π^\pm . Let then p_2 denote the four-momentum of the π^+ and p_3 that of the π^- of the interacting $[\pi^+\pi^-]$ pair in the B rest frame. One has $p_B = p_1 + p_2 + p_3$ and we introduce the invariants $s_{ij} = (p_i + p_j)^2$ for $i, j = 1, 2, 3$ with $i < j$. For the $B^- \rightarrow \pi^- [\pi^+\pi^-]_{S,P,D}$ amplitude, we work in the center of mass frame of the $\pi^+\pi^-$ pair of pions with respective four-momenta p_2 and p_3 (or p_1 and p_2 for the symmetrized amplitudes). These two pions will be either in a relative S , P or D state. In the following we derive the amplitudes for the $B^- \rightarrow \pi^- [\pi^+\pi^-]_{S,P,D}$ processes. The transcription to the $B^+ \rightarrow \pi^+ [\pi^+\pi^-]_{S,P,D}$ processes is straightforward. Applying the QCD factorization formula for the $B^- \rightarrow \pi^- [\pi^+\pi^-]_{S,P,D}$ process, the matrix elements of the effective weak Hamiltonian (1) can be written as [7]

$$\begin{aligned} & \langle \pi^-(p_1) [\pi^+(p_2)\pi^-(p_3)]_{S,P,D} | H_{eff} | B^-(p_B) \rangle = \\ & \frac{G_F}{\sqrt{2}} \sum_{p=u,c} \lambda_p \langle \pi^- [\pi^+\pi^-]_{S,P,D} | T_p | B^- \rangle, \end{aligned} \quad (3)$$

to which must be added the symmetrized term

$\langle \pi^-(p_3)[\pi^+(p_2)\pi^-(p_1)]_{S,P,D}|H_{eff}|B^-(p_B)\rangle$. With $M_1 \equiv \pi^-$ and $M_2 \equiv [\pi^+\pi^-]_{S,P}$ or $M_1 \equiv [\pi^+\pi^-]_{S,P,D}$ while $M_2 \equiv \pi^-$, one has

$$\begin{aligned}
\langle \pi^- [\pi^+\pi^-]_{S,P,D}|T_p|B^- \rangle &= \langle \pi^- [\pi^+\pi^-]_{S,P,D} | \\
&\left\{ a_1(M_1M_2)\delta_{pu}(\bar{u}b)_{V-A} \otimes (\bar{d}u)_{V-A} \right. \\
&+ a_2(M_1M_2)\delta_{pu}(\bar{d}b)_{V-A} \otimes (\bar{u}u)_{V-A} \\
&+ a_3(M_1M_2) \sum_q (\bar{d}b)_{V-A} \otimes (\bar{q}q)_{V-A} \\
&+ a_4^p(M_1M_2) \sum_q (\bar{q}b)_{V-A} \otimes (\bar{d}q)_{V-A} \\
&+ a_5(M_1M_2) \sum_q (\bar{d}b)_{V-A} \otimes (\bar{d}q)_{V+A} \\
&+ a_6^p(M_1M_2) \sum_q (-2)(\bar{q}b)_{sc-ps} \otimes (\bar{d}q)_{sc+ps} \\
&+ a_7(M_1M_2) \sum_q (\bar{d}b)_{V-A} \otimes \frac{3}{2}e_q(\bar{q}q)_{V+A} \\
&+ a_8^p(M_1M_2) \sum_q (-2)(\bar{q}b)_{sc-ps} \otimes \frac{3}{2}e_q(\bar{d}q)_{sc+ps} \\
&+ a_9(M_1M_2) \sum_q (\bar{d}b)_{V-A} \otimes \frac{3}{2}e_q(\bar{q}q)_{V-A} \\
&\left. + a_{10}^p(M_1M_2) \sum_q (\bar{q}b)_{V-A} \otimes \frac{3}{2}e_q(\bar{d}q)_{V-A} \right\} \\
&| B^- \rangle, \tag{4}
\end{aligned}$$

where a_j^p are effective QCDF coefficients.

In Eq.(4), $(\bar{q}_1q_2)_{V\mp A} = \bar{q}_1\gamma_\mu(1\mp\gamma_5)q_2$, $(\bar{q}_1q_2)_{sc\pm ps} = \bar{q}_1(1\pm\gamma_5)q_2$ and e_q denotes the electric charge of the quark q in units of the elementary charge e . The sum on the index q runs over u and d and the summation over the color degree of freedom has been performed. The notations sc and ps stand for scalar and pseudoscalar, respectively.

At next-to-leading order (NLO) in the strong coupling constant α_s , the general expression of the a_i^p quantities in terms of effective Wilson coefficients is [9]

$$a_i^p(M_1 M_2) = \left(C_i + \frac{C_{i\pm 1}}{N_C} \right) N_i(M_2) + \frac{C_{i\pm 1}}{N_C} \frac{C_F \alpha_s}{4\pi} [V_i(M_2) + \frac{4\pi^2}{N_C} H_i(M_1 M_2)] + P_i^p(M_2), \quad (5)$$

where the upper (lower) signs apply when the index i is odd (even), N_C is the number of colors, $N_C = 3$ and $C_F = (N_C^2 - 1)/2N_C$. The sums over the color degree of freedom have been performed in Eq. (4). Note that in the leading-order (LO) contribution $N_i(M_2) = 0$ for $M_2 = [\pi^+ \pi^-]_P$ and $i = 6, 8$, otherwise $N_i(M_2) = 1$. The NLO quantities $V_i(M_2)$ arise from one loop vertex corrections, $H_i(M_1 M_2)$ from hard spectator scattering interactions and $P_i^p(M_2)$ from penguin contractions. Here the meson M_2 is the meson which does not include the spectator quark of the B meson. The superscript p in $a_i^p(M_1 M_2)$ is to be omitted for $i = 1, 2, 3, 5, 7$ and 9 since the penguin corrections are equal to zero in these cases. In our calculation we shall not include the NLO hard scattering corrections nor the annihilation contributions which require the introduction of four phenomenological parameters to regularize end point divergences related to asymptotic wave functions [9]. Although we are aware that such contributions might be important, this would bring, at this stage of analysis, too many free parameters.

In Eq. (4) the symbol \otimes indicates that the different components of the matrix elements $\langle \pi^- [\pi^+ \pi^-]_{S,P,D} | T_p | B^- \rangle$ are to be calculated in the factorized form,

$$\begin{aligned} & \langle \pi^-(p_1) [\pi^+(p_2) \pi^-(p_3)]_{S,P,D} | j_1 \otimes j_2 | B^-(p_B) \rangle \\ & \equiv \langle [\pi^+ \pi^-]_{S,P,D} | j_1 | B^- \rangle \langle \pi^- | j_2 | 0 \rangle \text{ or } \langle \pi^- | j_1 | B^- \rangle \langle [\pi^+ \pi^-]_{S,P} | j_2 | 0 \rangle, \quad (6) \end{aligned}$$

since we neglect B^- annihilation contributions which are expected to be small [6]. Furthermore, as for the hard scattering corrections, their evaluation [9] introduces two phenomenological parameters. In Eq. (6) j_1 and j_2 denote the appropriate quark currents entering in Eq. (4). Note that, in our approach, in the evaluation of the long distance matrix element $\langle [\pi^+ \pi^-]_{S,P,D} | j_1 | B^- \rangle$, we make the hypothesis that the transitions of B^- to the $[\pi^+ \pi^-]_{S,P,D}$ states go first through intermediate meson resonances $R_{S,P,D}$ which then decay into a $\pi^+ \pi^-$ pair. We describe these decays by a vertex function modeled by assuming them to be proportional to the pion scalar or vector form factors or to a relativistic Breit-Wigner formula, respectively. For the short distance part of the decay amplitudes proportional to a combination of the effective coefficients $a_i^p(M_1 M_2)$ it can be seen that for terms coming from the first line of the right hand side of

Eq. (6) $M_1 \equiv [\pi^+\pi^-]_{S,P,D}$, $M_2 \equiv \pi^-$ and for those from the second line $M_1 \equiv \pi^-$ while $M_2 \equiv [\pi^+\pi^-]_{S,P}$, the $[\pi^+\pi^-]_D$ transition to the vacuum being zero with the involved bilinear quark current j_2 in Eq. (6). In the following, when $M_2 \equiv [\pi^+\pi^-]_{S,P}$, we assume that the NLO corrections $V_i(M_2)$ and $P_i^p(M_2)$ are evaluated at the meson resonances $R_{S,P}$ position. Here we take $R_P \equiv \rho(770)^0$ and $R_S \equiv f_0(980)$. A similar approximation has been applied in Refs. [3, 4] for the $[K\pi]_{S,P}$ states with $R_P \equiv K^*(892)$ and $R_S \equiv K_0^*(1430)$.

Introducing the following short distance terms, with $L \equiv S, P, D$ and with $R_D \equiv f_2(1270)$,

$$u(R_L\pi^-) = \lambda_u \left\{ a_1(R_L\pi^-) + a_4^u(R_L\pi^-) + a_{10}^u(R_L\pi^-) - [a_6^u(R_L\pi^-) + a_8^u(R_L\pi^-)] r_\chi^\pi \right\} + \lambda_c \left\{ a_4^c(R_L\pi^-) + a_{10}^c(R_L\pi^-) - [a_6^c(R_L\pi^-) + a_8^c(R_L\pi^-)] r_\chi^\pi \right\}, \quad (7)$$

$$v(\pi^- R_S) = \lambda_u [-2a_6^u(\pi^- R_S) + a_8^u(\pi^- R_S)] + \lambda_c [-2a_6^c(\pi^- R_S) + a_8^c(\pi^- R_S)], \quad (8)$$

and

$$w(\pi^- R_P) = \lambda_u \left\{ a_2(\pi^- R_P) - a_4^u(\pi^- R_P) + \frac{3}{2} [a_7(\pi^- R_P) + a_9(\pi^- R_P)] + \frac{1}{2} a_{10}^u(\pi^- R_P) \right\} + \lambda_c \left\{ -a_4^c(\pi^- R_P) + \frac{3}{2} [a_7(\pi^- R_P) + a_9(\pi^- R_P)] + \frac{1}{2} a_{10}^c(\pi^- R_P) \right\}, \quad (9)$$

one obtains, from Eqs. (3), (4) and (6), the following S -, P - and D -wave matrix elements

$$\sum_{p=u,c} \lambda_p \langle \pi^-(p_1) [\pi^+(p_2) \pi^-(p_3)]_S | T_p | B^- \rangle = X_S u(R_S \pi^-) + Y_S v(\pi^- R_S), \quad (10)$$

$$\sum_{p=u,c} \lambda_p \langle \pi^-(p_1) [\pi^+(p_2) \pi^-(p_3)]_P | T_p | B^- \rangle = X_P u(R_P \pi^-) + Y_P w(\pi^- R_P), \quad (11)$$

$$\sum_{p=u,c} \lambda_p \langle \pi^-(p_1) [\pi^+(p_2) \pi^-(p_3)]_D | T_p | B^- \rangle = X_D u(R_D \pi^-). \quad (12)$$

In Eq. (7) the chiral factor r_χ^π is given by $r_\chi^\pi = 2m_\pi^2 / [(m_b + m_u)(m_u + m_d)]$, m_u and m_d being the u and d quark masses, respectively. The long distance functions $X_{S,P,D}$ and $Y_{S,P}$, evaluated in Appendix A, read

$$\begin{aligned} X_S &\equiv \langle [\pi^+(p_2) \pi^-(p_3)]_S | (\bar{u}b)_{V-A} | B^- \rangle \langle \pi^-(p_1) | (\bar{d}u)_{V-A} | 0 \rangle \\ &= -\sqrt{\frac{2}{3}} \chi_S f_\pi (M_B^2 - s_{23}) F_0^{BR_S}(m_\pi^2) \Gamma_1^{n*}(s_{23}), \end{aligned} \quad (13)$$

$$\begin{aligned} Y_S &\equiv \langle \pi^-(p_1) | (\bar{d}b)_{sc-ps} | B^- \rangle \langle [\pi^+(p_2) \pi^-(p_3)]_S | (\bar{d}d)_{sc+ps} | 0 \rangle \\ &= \sqrt{\frac{2}{3}} B_0 \frac{M_B^2 - m_\pi^2}{m_b - m_d} F_0^{B\pi}(s_{23}) \Gamma_1^{n*}(s_{23}), \end{aligned} \quad (14)$$

$$\begin{aligned} X_P &\equiv \langle [\pi^+(p_2) \pi^-(p_3)]_P | (\bar{u}b)_{V-A} | B^- \rangle \langle \pi^-(p_1) | (\bar{d}u)_{V-A} | 0 \rangle \\ &= N_P \frac{f_\pi}{f_{R_P}} (s_{13} - s_{12}) A_0^{BR_P}(m_\pi^2) F_1^{\pi\pi}(s_{23}), \end{aligned} \quad (15)$$

$$\begin{aligned} Y_P &\equiv \langle \pi^-(p_1) | (\bar{d}b)_{V-A} | B^- \rangle \langle [\pi^+(p_2) \pi^-(p_3)]_P | (\bar{u}u)_{V-A} | 0 \rangle \\ &= (s_{13} - s_{12}) F_1^{B\pi}(s_{23}) F_1^{\pi\pi}(s_{23}), \end{aligned} \quad (16)$$

$$\begin{aligned} X_D &\equiv \langle [\pi^+(p_2) \pi^-(p_3)]_D | (\bar{u}b)_{V-A} | B^- \rangle \langle \pi^-(p_1) | (\bar{d}u)_{V-A} | 0 \rangle \\ &= -\frac{f_\pi}{\sqrt{2}} F^{BR_D}(m_\pi^2) \sqrt{\frac{2}{3}} \frac{G_{f_2 D}(s_{12}, s_{23})}{m_{R_D}^2 - s_{23} - im_{R_D} \Gamma(s_{23})}, \end{aligned} \quad (17)$$

The different quantities entering the above equations are discussed below.

The S -wave strength parameter χ_S [Eq. (13)] will be fitted together with the correction P -wave parameter N_P [Eq. (15)]. The deviation of N_P from 1 corresponds to the possible variation of the strength of this P -wave amplitude proportional to f_π/f_{R_P} [compare Eqs. (A.7) and (A.19)].

Three scalar-isoscalar f_0 resonances, viz. $f_0(600)$, $f_0(980)$ and $f_0(1400)$, are present in the $\pi\pi$ effective mass range, $m_{\pi\pi}$, considered here. Since some of them are wide, like $f_0(600)$, one could have a possible R_S dependence in χ_S . The transition form factor from B to R_S , $F_0^{BR_S}(m_\pi^2)$, could also depend on $m_{\pi\pi}$. However, one expects these dependences to be weaker than the effective mass dependence of the pion scalar form factor, $\Gamma_1^{n*}(s_{23})$, in which all these resonances are incorporated. Therefore we assume that χ_S and $F_0^{BR_S}(m_\pi^2)$ are constant. This hypothesis will be assessed by the quality of the fit obtained with our model. We shall take $R_S \equiv f_0(980)$ for the evaluation of $F_0^{BR_S}(m_\pi^2)$ and we use $F_0^{BR_S}(m_\pi^2) = 0.13$ [19].

For the pion decay constant we take $f_\pi = 0.1304$ GeV [18]. The R_P decay constant is denoted by f_{R_P} and the B -meson mass by M_B . Since the $\pi^+\pi^-$ P -wave is largely dominated by the $\rho(770)$ meson we choose $f_{R_P} = f_\rho = 0.209$ GeV [9]. The quantity $B_0 = -2 \langle 0|\bar{q}q|0\rangle/f_\pi^2$ is proportional to the quark condensate. We calculate it as $B_0 \simeq m_\pi^2/(m_u + m_d)$. At the renormalization scale $\mu = m_b/2$ we use $m_b = 4.9$ GeV and $m_u = m_d = 0.005$ GeV. For the transition form factor between the B meson and R_P state we set $A_0^{BR_P}(m_\pi^2) = 0.37$ [20].

For the $B\pi$ scalar and vector transition form factors $F_0^{B\pi}(s)$ and $F_1^{B\pi}(s)$, we use the following light-cone sum rule parametrization developed in Appendix A of Ref. [21], viz.

$$F_0^{B\pi}(s) = \frac{0.258}{1 - s/s_0}, \quad (18)$$

$$F_1^{B\pi}(s) = \frac{0.744}{1 - s/M_{B^*}^2} - \frac{0.486}{1 - s/s_1}, \quad (19)$$

with $s_0 = 33.81$ GeV², $M_{B^*} = 5.32$ GeV and $s_1 = 40.73$ GeV². The pion non-strange scalar and vector form factors $\Gamma_1^{n^*}(s)$ and $F_1^{\pi\pi}(s)$ will be discussed in the next section. Note that [22]

$$\Gamma_1^{n^*}(s) = \frac{\sqrt{3}}{2B_0} \langle [\pi^+\pi^-]_S | \bar{n}n | 0 \rangle, \quad (20)$$

with $\bar{n}n = \frac{1}{\sqrt{2}}(\bar{u}u + \bar{d}d)$.

The transition form factor between the B meson and the R_D state $F^{BR_D}(m_\pi^2)$ is not well known [23], so it will be taken as a free parameter to be fitted. The expressions of the tensor angular distribution factor $D(s_{12}, s_{23})$ and of the R_D mass dependence width $\Gamma(s_{23})$, similar to those used for the $f_2(1270)$ contribution in the BABAR Collaboration Dalitz plot analysis [5], are displayed in Sec. A.5 of the Appendix A. The expression of the $f_2(1270)$ coupling to $\pi\pi$, G_{f_2} , is also given there.

In summary, from the S -, P - and D -wave matrix elements (10), (11 and (12), we obtain the total symmetrized amplitude for the $B^- \rightarrow \pi^+\pi^-\pi^-$ decay as

$$\begin{aligned} \mathcal{M}_{sym}^-(s_{12}, s_{23}) = & \frac{1}{\sqrt{2}} [\mathcal{M}_S^-(s_{12}) + \mathcal{M}_S^-(s_{23}) + \mathcal{M}_P^-(s_{12})(s_{13} - s_{23}) \\ & + \mathcal{M}_P^-(s_{23})(s_{13} - s_{12}) + \mathcal{M}_D^-(s_{12})D(s_{23}, s_{12}) + \mathcal{M}_D^-(s_{23})D(s_{12}, s_{23})], \end{aligned} \quad (21)$$

with

$$\begin{aligned} \mathcal{M}_S^-(s_{ij}) = & \frac{G_F}{\sqrt{3}} \left[-\chi_S f_\pi (M_B^2 - s_{ij}) F_0^{BR_S}(m_\pi^2) u(R_S \pi^-) \right. \\ & \left. + B_0 \frac{M_B^2 - m_\pi^2}{m_b - m_d} F_0^{B\pi}(s_{ij}) v(\pi^- R_S) \right] \Gamma_1^{n^*}(s_{ij}), \end{aligned} \quad (22)$$

$$\mathcal{M}_P^-(s_{ij}) = \frac{G_F}{\sqrt{2}} \left[N_P \frac{f_\pi}{f_{R_P}} A_0^{BR_P}(m_\pi^2) u(R_P \pi^-) + F_1^{B\pi}(s_{ij}) w(\pi^- R_P) \right] F_1^{\pi\pi}(s_{ij}), \quad (23)$$

and

$$\mathcal{M}_D^-(s_{ij}) = -\frac{G_F}{\sqrt{3}} u(R_D \pi^-) \frac{f_\pi}{\sqrt{2}} F^{BR_D}(m_\pi^2) \frac{G_{f_2}}{m_{R_D}^2 - s_{ij} - im_{R_D}} \Gamma(s_{ij}). \quad (24)$$

For the fully symmetrized $B^+ \rightarrow \pi^+ \pi^- \pi^+$ decay amplitude we have

$$\begin{aligned} \mathcal{M}_{sym}^+(s_{12}, s_{23}) = & \frac{1}{\sqrt{2}} \left[\mathcal{M}_S^+(s_{12}) + \mathcal{M}_S^+(s_{23}) + \mathcal{M}_P^+(s_{12})(s_{13} - s_{23}) \right. \\ & \left. + \mathcal{M}_P^+(s_{23})(s_{13} - s_{12}) + \mathcal{M}_D^+(s_{12})D(s_{23}, s_{12}) + \mathcal{M}_D^+(s_{23})D(s_{12}, s_{23}) \right], \end{aligned} \quad (25)$$

with

$$\mathcal{M}_{S,P,D}^+(s_{ij}) = \mathcal{M}_{S,P,D}^-(s_{ij}, \lambda_u \rightarrow \lambda_u^*, \lambda_c \rightarrow \lambda_c^*, B^- \rightarrow B^+). \quad (26)$$

3. Scalar and vector form factors

As shown in Ref. [24] the full knowledge of strong interaction meson-meson form factors is available if the meson-meson interaction is known at all energies. The calculation of the S - and P -wave amplitudes (22) and (23) requires the values of the scalar and vector $B\pi$, $B(\pi\pi)$ and pion form factors. The knowledge of the $B \rightarrow \pi$ and $B \rightarrow [\pi\pi]_{S,P}$ transition form factors is needed far below the $B\pi$ and $B[\pi\pi]_{S,P}$ scattering region. One has then to rely on theoretical models constrained by experiment, as we do here for the $B[\pi\pi]_S$ form factor, using the value (see above in the previous section) determined in Ref. [19]. One could also use covariant light-front model, like that of Ref. [25] or, if available, semi-leptonic decay analysis results. For the $B\pi$ form factors we take the QCD light-cone sum rule results of Ref. [21] recalled above in Eqs. (18) and (19). The special case of the pion form factors is developed below.

3.1. The pion scalar form factor

In the $\pi\pi$ case, the low-energy S wave being known and modeling the high-energy part one can rely on the Muskhelishvili-Omnès equations [26] to build up the pion scalar form factors. Their evaluation from these equations has been discussed in Ref. [27] and followed and developed in Ref. [28]. However here, we shall use another approach, initiated in Ref. [22] and applied, using a different $\pi\pi$ scattering matrix, in Ref. [1]. Extending this last work by introducing three channels and keeping the off-shell contributions, the pion scalar form factor $\Gamma_1^{n*}(s)$ entering in the S -wave amplitude Eq. (22) is modeled according to the following relativistic three coupled-channel equations

$$\Gamma_i^{n*}(s) = R_i^n(E) + \sum_{j=1}^3 R_j^n(E) H_{ij}(E), \quad i = 1, 2, 3, \quad (27)$$

with

$$H_{ij}(E) = \int \frac{d^3p}{(2\pi)^3} T_{ij}(E, k_i, p) \frac{1}{E - 2\sqrt{p^2 + m_j^2} + i\epsilon} \frac{k_j^2 + \kappa^2}{p^2 + \kappa^2}, \quad (28)$$

where E represents the total energy, i.e., in the $\pi\pi$ center of mass, $E = \sqrt{s}$ and p is the off-shell momentum. In Eqs (27) and (28), the indices $i, j = 1, 2, 3$ refer to the $\pi\pi$, $K\bar{K}$ and effective $(2\pi)(2\pi)$ channels, respectively. The center of mass momenta are $k_j = \sqrt{s/4 - m_j^2}$, with $m_1 = m_\pi$, $m_2 = m_K$ and $m_3 = m_{(2\pi)}$. The T matrix is the corresponding three-channel two-body scattering matrix. Here we use the solution A of the three-coupled channel model of Refs. [29, 30], where the effective $m_{(2\pi)} = 700$ MeV. The functions $R_i^n(E)$ are the production functions responsible for the formation of the meson pairs before their scattering. From Eqs. (27) and (28) one can check that

$$Im \Gamma_i^{n*}(s) = - \sum_{j=1}^3 \frac{k_j \sqrt{s}}{8\pi} T_{ji}^*(E, k_j, k_i) \Gamma_j^{n*}(s) \theta(\sqrt{s} - 2m_j). \quad (29)$$

This is the same unitary relation as that of the corresponding Muskhelishvili-Omnès pion scalar form factors constructed in Ref. [28] [see Eq. (28) therein].

In Eq. (28) the regulator function $(k_j^2 + \kappa^2)/(p^2 + \kappa^2)$, which reduces to 1 on-shell ($k_j = p$), ensures the convergence of the integral. The range parameter κ will be fitted to data. The choice of a separable form for the interaction yields analytic expressions for the T matrix elements. One

introduces a rank-2 separable potential in the $\pi\pi$ channel and a rank-1 separable potential in the $K\bar{K}$ and in the $(2\pi)(2\pi)$ ones. According to the formalism developed in Ref. [31] and applied in Ref. [29] one has for the T matrix elements:

$$\begin{aligned}
T_{11}(E, p, k_1) &= g_0(k_1)t_{00}(E)g_0(p) + g_1(k_1)t_{11}(E)g_1(p) + g_0(k_1)t_{10}(E)g_1(p) \\
&\quad + g_1(k_1)t_{01}(E)g_0(p), \\
T_{21}(E, p, k_1) &= g_0(k_1)t_{02}(E)g_2(p) + g_1(k_1)t_{12}(E)g_2(p), \\
T_{31}(E, p, k_1) &= g_0(k_1)t_{03}(E)g_3(p) + g_1(k_1)t_{13}(E)g_3(p),
\end{aligned} \tag{30}$$

where

$$\begin{aligned}
g_0(k_1) &= \sqrt{\frac{4\pi}{m_\pi}} \frac{1}{k_1^2 + \beta_0^2}, \\
g_j(k_i) &= \sqrt{\frac{4\pi}{m_i}} \frac{1}{k_i^2 + \beta_j^2}, \quad j = 1, 2, 3.
\end{aligned} \tag{31}$$

The parameters β_j , $j = 0, 1, 2, 3$, of the separable form of the scattering T matrix are given in Table 1 of Ref. [29] (fit A).

One can extend the expressions of the reduced symmetric $t(E)$ matrix elements given in terms of the separable potential parameters in Appendix A of Ref. [31] to the case of Ref. [29] which we use here. The Yamaguchi form [32] of the $g_0(p)$ and $g_i(p)$ (31) in the T matrix elements (30) leads the following analytic expression for $\Gamma_i^{n*}(s)$ in Eq. (27)

$$\begin{aligned}
\Gamma_1^{n*}(s) &= R_1^n(E) + R_1^n(E)\{[t_{00}(E)g_0(k_1) + t_{01}(E)g_1(k_1)]g_0(k_1)F_{10}(k_1) + \\
&\quad [t_{11}(E)g_1(k_1) + t_{10}(E)g_0(k_1)]g_1(k_1)F_{11}(k_1)\} + \\
&\quad R_2^n(E)[g_0(k_1)t_{02}(E) + g_1(k_1)t_{12}(E)]g_2(k_2)F_{22}(k_2) + \\
&\quad R_3^n(E)[g_0(k_1)t_{03}(E) + g_1(k_1)t_{13}(E)]g_3(k_3)F_{33}(k_3),
\end{aligned} \tag{32}$$

where

$$\begin{aligned}
F_{10}(k_1) &= \frac{I_{1,0}(k_1)}{g_0(k_1)h_0(k_1)}, \\
F_{11}(k_1) &= \frac{I_{1,1}(k_1)}{g_1(k_1)h_1(k_1)}, \\
F_{22}(k_2) &= \frac{I_{2,2}(k_2)}{g_2(k_2)h_2(k_2)}, \\
F_{33}(k_3) &= \frac{I_{3,3}(k_3)}{g_3(k_3)h_3(k_3)},
\end{aligned} \tag{33}$$

with

$$\begin{aligned}
h_i(k_i) &= \sqrt{\frac{4\pi}{m_i}} \frac{1}{k_i^2 + \kappa^2}, \quad i = 1, 2, 3, \\
h_0(k_1) &= h_1(k_1),
\end{aligned} \tag{34}$$

and

$$I_{i,j}(k_i) = \int \frac{d^3p}{(2\pi)^3} g_j(p) \frac{1}{E - 2\sqrt{p^2 + m_i^2} + i\epsilon} h_i(p), \tag{35}$$

where $E = 2\sqrt{k_i^2 + m_i^2}$, $i = 1, 2, 3$. The analytical expression for these integrals can be found in Appendix A of Ref. [31].

As in Ref. [22] one constrains the $\Gamma_i^{n*}(s)$ to satisfy the low energy behavior given by next-to-leading order one loop calculation in chiral perturbation theory (ChPT). One writes the expansion at low s as

$$\Gamma_i^n(s) \cong d_i^n + f_i^n s, \quad i = 1, 2, 3, \tag{36}$$

with real coefficients, $\Gamma_i^n(s)$ being real below the $\pi\pi$ threshold. Using the expressions obtained in NLO in ChPT for the $\Gamma_i^{n*}(s)$ given in Refs. [22, 33] one gets,

$$\begin{aligned}
d_1^n &= \sqrt{\frac{3}{2}} \left[1 + \frac{16m_\pi^2}{f^2} (2L_8^r - L_5^r) + 8 \frac{2m_K^2 + 3m_\pi^2}{f^2} (2L_6^r - L_4^r) \right. \\
&\quad \left. + \frac{m_\pi^2}{36\pi^2 f^2} + \frac{m_\pi^2}{16\pi^2 f^2} \log \frac{m_\pi^2}{\nu^2} - \frac{1}{96\pi^2 f^2} \left(\frac{m_\pi^2}{3} + m_\eta^2 \right) \log \frac{m_\eta^2}{\nu^2} \right], \\
f_1^n &= \sqrt{\frac{3}{2}} \left[\frac{4}{f^2} (2L_4^r + L_5^r) - \frac{1}{16\pi^2 f^2} \left(1 + \log \frac{m_\pi^2}{\nu^2} \right) \right. \\
&\quad \left. - \frac{1}{64\pi^2 f^2} \left(1 + \log \frac{m_K^2}{\nu^2} \right) - \frac{m_\pi^2}{192\pi^2 f^2} \left(\frac{1}{m_\pi^2} - \frac{1}{9m_\eta^2} \right) \right], \quad (37)
\end{aligned}$$

and

$$\begin{aligned}
d_2^n &= \frac{1}{\sqrt{2}} \left[1 + \frac{m_\eta^2}{48\pi^2 f^2} \log \frac{m_\eta^2}{\nu^2} + \frac{16m_K^2}{f^2} (2L_8^r - L_5^r) \right. \\
&\quad \left. + 8 \frac{6m_K^2 + m_\pi^2}{f^2} (2L_6^r - L_4^r) + \frac{m_K^2}{72\pi^2 f^2} \left(1 + \log \frac{m_\eta^2}{\nu^2} \right) \right], \\
f_2^n &= \frac{1}{\sqrt{2}} \left[\frac{4}{f^2} (2L_4^r + L_5^r) - \frac{1}{64\pi^2 f^2} \left(1 + \log \frac{m_\eta^2}{\nu^2} \right) - \frac{m_K^2}{432\pi^2 f^2} \frac{1}{m_\eta^2} \right. \\
&\quad \left. - \frac{3}{64\pi^2 f^2} \left(1 + \log \frac{m_K^2}{\nu^2} \right) - \frac{3}{64\pi^2 f^2} \left(1 + \log \frac{m_\pi^2}{\nu^2} \right) \right], \quad (38)
\end{aligned}$$

ν being the scale of dimensional regularization and $f = f_\pi/\sqrt{2}$. Furthermore for the ChPT low-energy constants, L_k^r , $k = 4, 5, 6, 8$, we use the recent determinations of lattice QCD at $\nu = 1$ GeV as given in Table X of Ref. [34]. For $f = 92.4$ MeV, we obtain $d_1^n = 1.1957$, $f_1^n = 3.1329$ GeV $^{-2}$, $d_2^n = 0.7193$ and $f_2^n = 1.6719$ GeV $^{-2}$. As in Ref. [28] we assume $\Gamma_3^n(0) = 0$ which leads to $d_3^n = 0$ and we also assume $f_3^n = 0$.

The real production functions are parametrized as

$$R_i^n(E) = \frac{\alpha_i^n + \tau_i^n E + \omega_i^n E^2}{1 + cE^4}, \quad i = 1, 2, 3, \quad (39)$$

the fitted parameter c controlling the high energy behavior. The other parameters, α_i^n , τ_i^n and ω_i^n are calculated by requiring that $\Gamma_i^n(s)$ in Eq. (27) has the low energy expansion Eq. (36). These nine parameters satisfy a linear system of nine equations displayed in Appendix B. Their numerical values, depending on the value of the range parameter κ [see Eq. (28)], will be given in Sec. 5.

3.2. The pion vector form factor

As for the scalar case one could use the Muskhelishvili-Omnès equations to build up the pion vector form factor. This was done in Ref. [3] for the $K\pi$ vector form factor. Here, noting that the knowledge of this form factor is required to describe the $\tau^- \rightarrow \pi^- \pi^0 \nu_\tau$ decay, we shall use the phenomenological model of the Belle Collaboration [35]. Fitting their high statistics data, they built the pion vector form factor $F_1^{\pi\pi}(s_{23})$ by including the contribution of the three vector resonances $\rho(770)$, $\rho(1450)$ and $\rho(1700)$. Here we use the parameters given in the third column of Table VII of Ref. [35].

4. Observables and data fitting

4.1. Physical observables

The symmetrized $B^- \rightarrow \pi_1^- \pi_2^+ \pi_3^-$ amplitude (21) depends on the two effective $\pi\pi$ masses, $m_{12} = \sqrt{s_{12}}$ and $m_{23} = \sqrt{s_{23}}$ of the Dalitz plot. In the center of mass of $\pi^-(p_1)$ and $\pi^+(p_2)$, the pion momenta fulfill the equations

$$\begin{aligned} |\vec{p}_1| &= \frac{1}{2} \sqrt{m_{12}^2 - 4m_\pi^2}, & |\vec{p}_2| &= |\vec{p}_1|, \\ |\vec{p}_3| &= \frac{1}{2m_{12}} \sqrt{\left[M_B^2 - (m_{12} + m_\pi)^2\right] \left[M_B^2 - (m_{12} - m_\pi)^2\right]}, \end{aligned} \quad (40)$$

and the cosine of the helicity angle θ between the direction of \vec{p}_2 and that of \vec{p}_3 reads

$$\cos \theta = \frac{1}{2|\vec{p}_2||\vec{p}_3|} \left[-m_{23}^2 + \frac{1}{2} (M_B^2 - m_{12}^2 + 3m_\pi^2) \right]. \quad (41)$$

For fixed values of the effective mass m_{12} , the variables $\cos \theta$ and m_{23} are equivalent.

The double differential $B^- \rightarrow \pi^- \pi^+ \pi^-$ branching fraction is

$$\frac{d^2\mathcal{B}^-}{dm_{12} d\cos\theta} = \frac{1}{\Gamma_B} \frac{m_{12} |\vec{p}_2| |\vec{p}_3|}{8(2\pi)^3 M_B^3} |\mathcal{M}_{sym}^-(s_{12}, s_{23})|^2, \quad (42)$$

where Γ_B is the total width of the B^- . Since the Dalitz plot is symmetric under the interchange of m_{12} and m_{23} , one can limit the integration range on m_{23} to the values larger than m_{12} ; hence, the differential effective mass distribution reads

$$\frac{d\mathcal{B}^-}{dm_{12}} = \int_{-1}^{\cos\theta_g} \frac{d^2\mathcal{B}^-}{dm_{12} d\cos\theta} d\cos\theta, \quad (43)$$

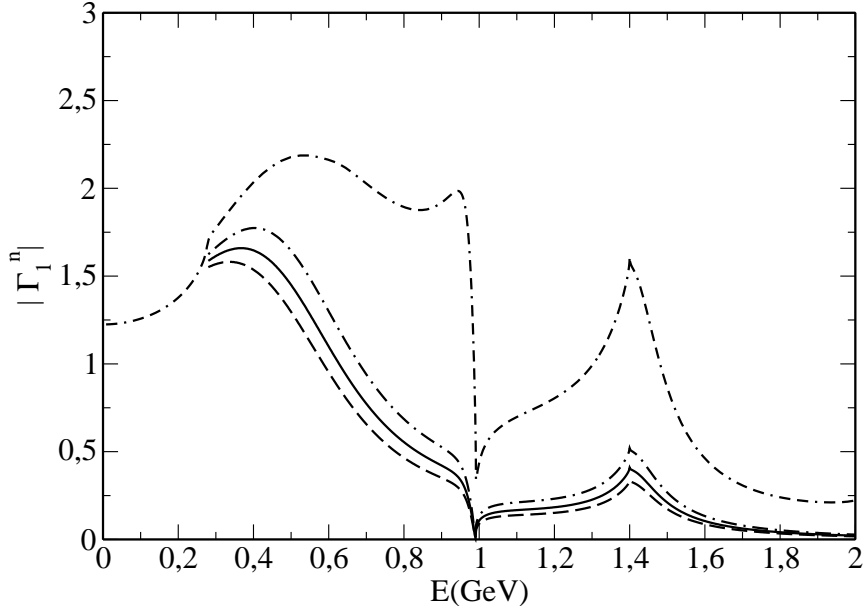


Fig. 1. Modulus of the pion scalar form factor Γ_1^n (solid line), obtained in our fit using the NLO a_i^p with $\kappa = 2$ GeV and for which the fitted parameter $c = (19.5 \pm 4.2)$ GeV $^{-4}$, compared to that calculated in Ref. [37] using the Muskhelishvili-Omnès equations (double-dash dot line). The dash-dot line (for $c = 15.3$ GeV $^{-4}$) and the dashed one (for $c = 23.7$ GeV $^{-4}$) represent the variation of the Γ_1^n modulus when c varies within its error band.

where $\cos \theta_g$ corresponds to the value of $\cos \theta$ in Eq. (41) with $m_{12} = m_{23}$, viz.,

$$\cos \theta_g = \frac{1}{4|\vec{p}_2||\vec{p}_3|} (M_B^2 - 3m_{12}^2 + 3m_\pi^2). \quad (44)$$

The variable m_{12} in Eq. (43) is also called the light (or minimal) effective mass m_{min} while m_{23} is the heavy (or maximal) effective mass, m_{max} . The $B^- \rightarrow \pi^- \pi^+ \pi^-$ branching fraction is then twice the integral of the differential branching fraction (43) over m_{12} .

4.2. Data fitting

We aim at describing the experimental $\pi^+ \pi^-$ distributions obtained by the BABAR Collaboration in the Dalitz plot analysis of the $B^\pm \rightarrow \pi^\pm \pi^\pm \pi^\mp$ decays [5]. Two different background distributions, related to the $q\bar{q}$ and the $B\bar{B}$ components, are subtracted from Fig. 4 of Ref. [5]. Six light effective $\pi^+ \pi^-$ mass distributions are extracted for B^+ and B^- decays with

a subdivision of the data into positive and negative values of the cosine of the helicity angle θ . For the B^+ and B^- distributions we reject two data points corresponding to the $\pi^+\pi^-$ effective masses equal to 485 and 515 MeV. Also two points at 470 and 530 MeV for the four mass distributions with $\cos\theta > 0$ or with $\cos\theta < 0$ are not taken into account. This is done to exclude the possible contribution of the decay processes $B^\pm \rightarrow K_S^0\pi^\pm$.

As a by-product of the background subtraction, five data points, with a small number of events, have negative values with small statistical errors. For these five data points we increase their errors to values corresponding to those of the points lying in a close vicinity. This is done at 1385 MeV for the B^- distribution, at 1475 MeV for the B^+ one, at 290 and 1610 MeV for the B^- distribution with $\cos\theta > 0$ and at 1490 MeV for the B^- one with $\cos\theta < 0$.

We perform a χ^2 fit to the 170 data points corresponding to the six invariant mass distributions described above. In addition, we include the experimental branching ratio for the $B^\pm \rightarrow \rho(770)^0\pi^\pm$, $\rho(770)^0 \rightarrow \pi^+\pi^-$ decay channel. The theoretical distributions are normalized to the number of experimental events in the analyzed range from 290 up to 1640 MeV. In the fits, done for a fixed value of the range parameter κ entering Eqs. (28) [see Sec. 5], the following four parameters were varied: the production functions $R_i^n(E)$ [Eq. (39)] parameter c , the real S -wave strength parameter χ_S , the real P -wave correction parameter N_P [Eq. (15)] and the transition form factor $F^{BRD}(m_\pi^2)$ [Eq. (17)].

5. Results and discussion

In the fits to the selected BABAR data as described in the previous section, the CKM matrix elements [see Eq. (2)] are calculated with $\lambda = 0.2257$, $A = 0.814$, $\bar{\rho} = 0.135$ and $\bar{\eta} = 0.349$ [18] which leads to $\lambda_u = 1.26 \times 10^{-3} - i 3.27 \times 10^{-3}$ and $\lambda_c = -9.35 \times 10^{-3} - i 1.72 \times 10^{-6}$. The LO contributions of the Wilson coefficients to the a_i^p Eq. (5) are given in the second and fourth columns of Table 1. The sum of the leading order coefficient plus the next-to-leading order vertex and penguin corrections for the a_i^p coefficients, entering into $u(R_{S,P}\pi^-)$ [Eq. (7)], $v(\pi^-R_S)$ [Eq. (8)] and $w(\pi^-R_P)$ [Eq. (9)], are displayed in columns three and five, respectively. It can be seen that the NLO corrections are relatively small except for the coefficient a_2 which, however, has only a small contribution to the decay amplitude. The corrections are calculated according to Refs. [7] and [9] using the Gegenbauer moments for pions taken from the Table 2 of Ref. [7] and the corresponding moments for the ρ meson from Table 1 of Ref. [36]. In the calculation of the coefficients $a_6^p(\pi^-R_S)$ and $a_8^p(\pi^-R_S)$, contributing to $v(\pi^-R_S)$, we apply the method explained in Appendix A of Ref. [11]. Here

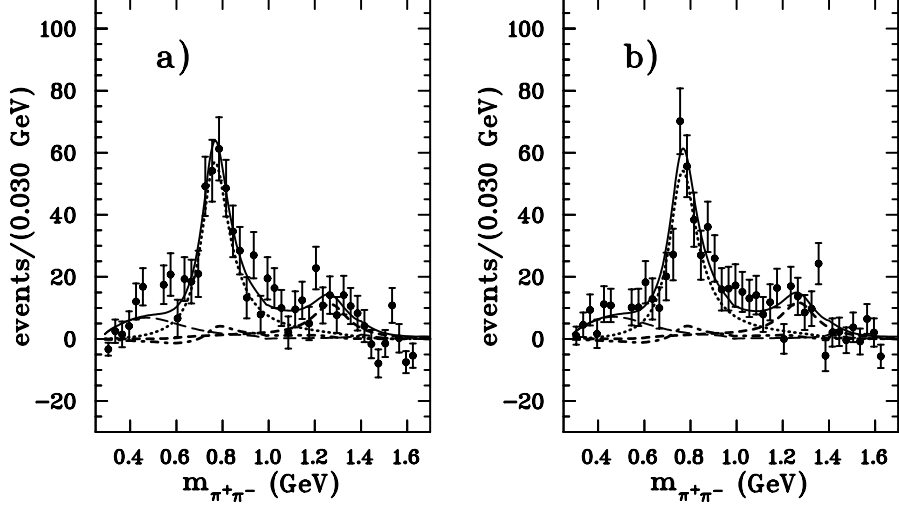


Fig. 2. The $\pi^+\pi^-$ light effective mass distributions from the fit to the BABAR experimental data [5], a) for the B^- decays and b) for the B^+ decays. The long-dash line represents the S -wave contribution of our model, the dot line that of the P wave, the short-dash line that of the D wave and the dot-dash line that of the interference term. The solid line corresponds to the sum of these contributions.

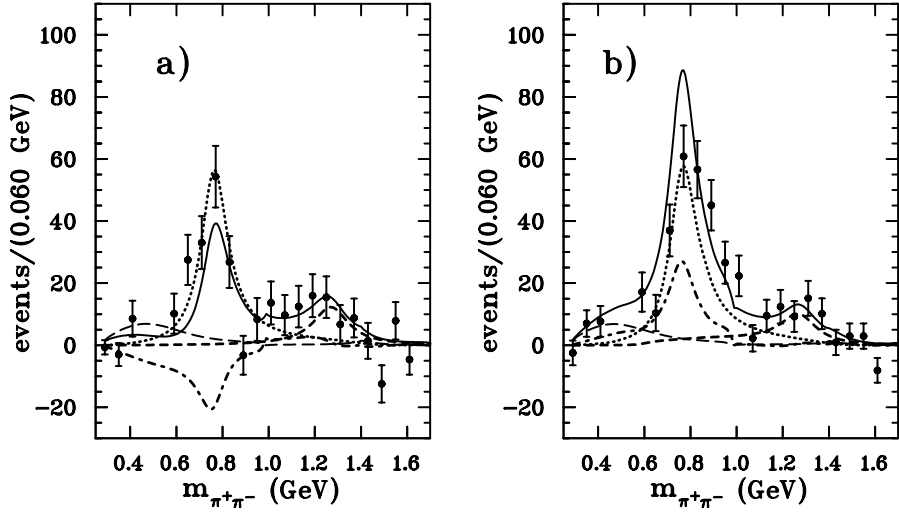


Fig. 3. As in Fig. 2 but for the B^- decays a) with $\cos\theta < 0$ and b) with $\cos\theta > 0$.

the renormalization scale $\mu = m_b/2$ and we take for the strong coupling constant $\alpha_s(m_b/2) = 0.303$.

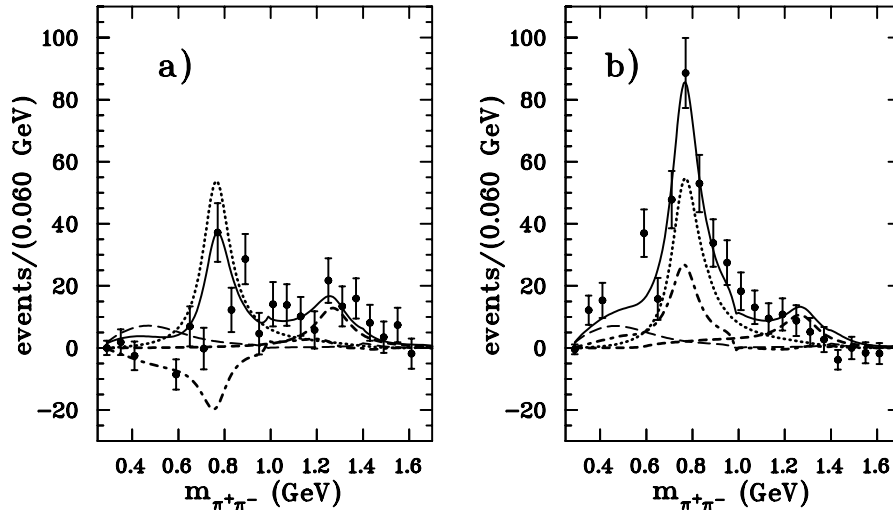


Fig. 4. As in Fig. 3 but for the B^+ decays.

Table 1. Leading order (LO) and next-to-leading order (NLO) coefficients $a_i^p(R_{S,P}\pi^-)$, $a_i^p(\pi^-R_S)$ (in parentheses) and $a_i^p(\pi^-R_P)$ [see Eq. (5)] entering into $u(R_{S,P}\pi^-)$ [Eq. (7)], $v(\pi^-R_S)$ [Eq. (8)] and $w(\pi^-R_P)$ [Eq. (9)], respectively. The NLO coefficients are the sum of the LO coefficients plus next-to-leading order vertex and penguin corrections. Here the renormalization scale is $\mu = m_b/2$. The superscript p is omitted for $i = 1, 2, 3, 5, 7$ and 9 , the penguin corrections being zero for these cases.

	$a_i^p(R_{S,P}\pi^-)$		$a_i^p(\pi^-R_{S,P})$	
	LO	NLO	LO	NLO
a_1	1.039	$1.071 + i0.03$		
a_2			0.084	$-0.041 - i0.114$
a_4^u	-0.044	$-0.032 - i0.019$	-0.044	$-0.032 - i0.019$
a_4^c	-0.044	$-0.039 - i0.007$	-0.044	$-0.039 - i0.007$
a_6^u	-0.062	$-0.057 - i0.017$	(-0.062)	($-0.075 - i0.017$)
a_6^c	-0.062	$-0.062 - i0.004$	(-0.062)	($-0.079 - i0.004$)
a_7			0.0001	$0.0 + i0.0001$
a_8^u	0.0007	$0.0008 + i0.0$	(0.0007)	($0.0007 + i0.0$)
a_8^c	0.0007	$0.0008 + i0.0$	(0.0007)	($0.0007 + i0.0$)
a_9			-0.0094	$-0.0097 - i0.0003$
a_{10}^u	-0.0009	$0.0006 + i0.0010$	-0.0009	$0.0006 + i0.0010$
a_{10}^c	-0.0009	$0.0006 + i0.0010$	-0.0009	$0.0006 + i0.0010$

There are five free parameters at our disposal. Two of them, the regulator range κ and the high energy cut-off c of the production functions

Table 2. Parameters of the production functions $R_i^n(E)$ Eq. (39) for $\kappa = 2$ GeV

i	α_i^n	τ_i^n (GeV $^{-1}$)	ω_i^n (GeV $^{-2}$)
1	0.7095	-0.2707	1.6251
2	0.5759	-0.0032	1.4171
3	1.003	0.3724	2.7427

[Eq. (39)] are linked to the determination of the S -wave Γ_1^n form factor. The other three, χ_S , N_P and $F^{BRD}(m_\pi^2)$ are related to the strength of the S , P and D amplitudes, respectively. The range κ should be larger than 0.8 GeV which is the on-shell pion momentum approximately equal to the half of the effective $m_{\pi\pi}$ upper limit ~ 1.64 GeV which we used. In our fits we find that the total χ^2 decreases slowly when κ decreases from the high value of 5 GeV. Here we fix the range parameter κ to be 2 GeV. We perform two fits for the full $S+P+D$ -wave amplitude calculated with the NLO and with the LO a_i^p coefficients. Hereafter the quoted results given inside parentheses correspond to the numbers obtained in the second fit. The quoted errors on our results come from the statistical errors in the experimental data.

A good overall agreement with BABAR's data is achieved with $c = 19.5 \pm 4.2$ (18.9 ± 4.1) GeV $^{-4}$, $\chi_S = -19.4 \pm 2.5$ (-19.8 ± 2.6) GeV $^{-1}$, $N_P = 1.122 \pm 0.034$ (1.015 ± 0.035) and $F^{BRD}(m_\pi^2) = 0.0977 \pm 0.0070$ (0.1010 ± 0.0072). The total χ^2 is equal to 231.6 (233.5) for the 171 experimental points of the fit. For both fits the branching fraction for the $B^\pm \rightarrow \rho(770)^0 \pi^\pm$, $\rho(770)^0 \rightarrow \pi^+ \pi^-$ decay is $(8.1 \pm 0.5) \times 10^{-6}$, to be compared with the BABAR Collaboration determination of $(8.1 \pm 0.5 \pm 1.2_{-1.1}^{+0.4}) \times 10^{-6} \approx (8.1 \pm 1.6) \times 10^{-6}$ from their isobar model analysis [5]. Note that for the LO fit we explain essentially the BABAR Collaboration's result without significant modification of the P wave normalization, the parameter $N_P \approx 1.02$ being close to 1. For the NLO fit, $N_P \approx 1.12 \pm 0.03$ and one can compare $N_P^2 - 1 \approx 25\%$ with the average 20% error of the experimental branching ratio.

The CP average total branching fraction of the $B^\pm \rightarrow \pi^\pm \pi^\mp \pi^\pm$ decays calculated in the NLO fit is equal to $(15.2 \pm 1.1) \times 10^{-6}$ to be compared to the measured value of $(15.2 \pm 0.6 \pm 1.2_{-0.3}^{+0.4}) \times 10^{-6}$ (table III of Ref. [5]). The branching fraction for the S wave equals to $(2.3 \pm 0.4) \times 10^{-6}$ and that for the D wave is $(2.8 \pm 0.4) \times 10^{-6}$. The latter value is larger than the branching fraction for the $f_2(1270)\pi^\pm$, $(0.9 \pm 0.2 \pm 0.1_{-0.1}^{+0.3}) \times 10^{-6}$, determined in Ref. [5]. In the experimental analysis the two resonances, namely $f_2(1270)$ and $f_0(1370)$, overlap to a large extent, which makes their separation difficult and some part of the branching fraction obtained for one resonance could have been attributed to the other one. The isobar model analysis of Ref. [5] gives $(2.9 \pm 0.5 \pm 0.5_{-0.5}^{+0.7}) \times 10^{-6}$ for the branching frac-

tion of $f_0(1370)\pi^\pm$. Then, the sum of the branching fractions for the two resonances equals to 3.8×10^{-6} . This value compares well with the branching fraction of 3.6×10^{-6} obtained by integrating our distribution in the $m_{\pi\pi}$ range between 1.0 and 1.64 GeV in which both $f_2(1270)$ and $f_0(1370)$ give their dominant contributions. In our model the D -wave contribution is dominant in this range. Let us note that the value we obtain for the transition form factor $F^{BRD}(m_\pi^2)$ is 29% larger than the value 0.076 given in Table 1 of Ref. [23] for the ISGW2 model. The S -wave contribution represents here as much as 15% of the total branching fraction. This contribution is of the same order as that of the $\rho(1450)$ and $\rho(1700)$ which also represents 15 % of the total P -wave contribution.

Before comparing our effective mass distributions to the experimental ones, we now give our result for the pion scalar form factor $\Gamma_1^n(s)$. With the fixed value of $\kappa = 2$ GeV used in the fits, one obtains for the α_i^n , τ_i^n and ω_i^n , $i = 1, 2, 3$, entering into Eq. (39), the values given in Table 2. Then, in Fig. 1, we show the modulus of the pion scalar form factor obtained using the NLO coefficients a_i^p for the fitted value of the parameter $c = (19.5 \pm 4.2 \text{ GeV})^{-4}$ together with its envelope when c varies within its error band. It is also compared to that of the scalar form factor calculated by Moussallam [37] solving the Muskhelishvili-Omnès equations [26] with a high-energy ansatz starting at 2 GeV and the same low-energy three coupled-channel scattering T-matrix as in our model (see Sec. 3.1). However, in his calculation the off-diagonal matrix elements $T_{13}(E, k_i, p)$ and $T_{23}(k_i, E, p)$ are set to zero in the unphysical region $E < 2m_3 = 1.4$ GeV. Let us remind here that the imaginary parts of these two pion form factors satisfy exactly the same relation given by Eq. (29). The functional dependence of both $\Gamma_1^{n*}(s)$ moduli is quite similar. It can be seen in Fig. 1 that, within our model, the needed $\Gamma_1^{n*}(s)$ is relatively well constrained. If we fix $\kappa = 3$ GeV then the fit to BABAR data gives $c = (30.4 \pm 6.6) \text{ GeV}^{-4}$, $\chi_S = (-20.2 \pm 2.9) \text{ GeV}^{-1}$ with a total χ^2 of 234.1. In this range of variation of the strongly correlated κ and c parameters, we have checked that the scalar form factor varies smoothly. The corresponding values of the strength parameter χ_S , being very close to -20 GeV^{-4} , are not sensitive to these variations. For $\kappa = 3$ GeV the values of the branching fractions for the different $\pi\pi$ waves stay within the error bands of those for the $\kappa = 2$ GeV case.

The threshold behavior of our pion form factor is governed by the chiral perturbation expansion Eq. (36). These ChPT constraints, not explicitly included in Moussallam's case, lead to $\Gamma_1^{n*}(s)$ moduli of both approaches to differ only slightly near the $\pi\pi$ threshold. Above the $\pi\pi$ threshold, there is a maximum corresponding to the $f_0(600)$ resonance, then close to 1 GeV a characteristic dip due to the $f_0(980)$ and finally, below the spike at 1.4 GeV related to the opening of the third channel, there is some enhance-

ment generated by the $f_0(1400)$ present in the $\pi\pi$ three-channel model used here [29, 30]. The third threshold energy equal to 1.4 GeV is a parameter representing twice the mass of the effective two-pion mass $m_{(2\pi)}$ used to account for the four pion decays of scalar mesons (see Ref. [29]). Thus, in nature there is no such sharp energy behavior. These characteristic features of the pion scalar form factor $\Gamma_1^n(s)$ are essential to obtain a good fit of the experimental effective mass distributions of the B^\pm to 3π decays.

The results of the fit on the experimental distributions, obtained using the NLO coefficients a_i^p in the $B^\pm \rightarrow \pi^\pm \pi^\mp \pi^\pm$ amplitudes, are displayed in Figs. 2, 3 and 4. The $\rho(770)$ -resonance contribution dominates the $\pi^+\pi^-$ spectrum, but that of the S -wave is non negligible. As seen, the S -wave part is sizable near 500 MeV which is related to the contribution of the scalar resonance $f_0(600)$, not explicitly included in the BABAR Dalitz plot analysis [5]. In the 1 GeV range the $f_0(980)$ resonance is not observed as a peak in the $\pi^+\pi^-$ spectrum. This fact is easily explained in our model since the decay amplitudes are proportional to the pion scalar form factor which has a dip near 1 GeV as seen in Fig. 1. Around 1.3 GeV there is a maximum coming from the contribution of the $f_2(1270)$ resonance. Near 1.4 GeV the $f_0(1400)$ scalar resonance [29, 30] gives only a tiny enhancement in the distributions.

Figure 2 exhibits a small CP asymmetry, the B^- and B^+ effective mass distributions being very close. Summing the number of experimental events in the $m_{\pi^+\pi^-}$ range between 290 and 1640 MeV one finds 616 events for the B^- decay and 606 for that of the B^+ . This leads to a CP asymmetry of $(0.8 \pm 4.8)\%$ which can be compared to the values of $(1.7 \pm 0.2)\%$ for the NLO fit and $(-0.06 \pm 0.08)\%$ for the LO fit. Taking into account the statistical error of 4.8% and adding to it a few percent systematic error one sees that both fits agree with experiment. Let us recall here the experimental value of the CP asymmetry $A_{CP} = (3.2 \pm 4.4 \pm 3.1_{-2.0}^{+2.5})\%$ for the total sample of $\pi^\pm \pi^\mp \pi^\pm$ events [5]. For the particular decay mode, namely for the B^\pm decay into $\rho(770)^0 \pi^\pm$, $\rho(770)^0 \rightarrow \pi^+\pi^-$, the isobar model analysis gives $A_{CP} = (18 \pm 7 \pm 5_{-14}^{+2})\%$, while from our model we get $3.6\% \pm 0.2\%$ ($-0.03\% \pm 0.001\%$). Note here that the asymmetries obtained for the fit corresponding to the amplitudes calculated with the real LO a_i^p coefficients are quite small as it could have been expected.

Figures 3 and 4 show a spectacular feature, namely that the interference term of the S , P and D waves is quite important under the $\rho(770)^0$ maximum. Here the S - P interference dominates. The sign of this interference term depends on the sign of $\cos\theta$, so the ρ peak is reduced for the negative values of $\cos\theta$ and enhanced for the positive values. This is a clear indication that the $\pi^+\pi^-$ effective mass distribution cannot be reproduced without the S -wave contribution. If we try to fit the data without the S -

wave amplitude then we obtain a poor fit with $\chi^2 = 316.3$. In this case the effective mass distributions are not well described below 600 MeV and also under the ρ maximum. One striking feature is that the interference terms allow an extremely good representation of the separate $\cos\theta < 0$ and $\cos\theta > 0$ spectra for the B^+ decays (Fig. 4) and yield for the full spectrum [Fig. 2b)] a χ^2/point of 1.07. The fit of the separate B^- spectra (Fig. 3) is less satisfactory whereas that of the full spectrum [Fig. 2a)] is almost perfect with a χ^2/point of 1.2.

6. Summary and outlook

The present paper is a continuation of our efforts [1, 2, 3, 4] in constraining theoretically the meson-meson final state strong interactions in hadronic charmless three-body B decays. If the strong interaction amplitudes are sufficiently well understood then one can improve the precision of the weak interaction amplitudes extracted from these reactions.

Our theoretical model for the $B^\pm \rightarrow \pi^\pm \pi^\mp \pi^\pm$ is based on the application of the QCD factorization [6, 7, 9, 13] to quasi two-body processes in which only two of the three produced pions interact strongly, forming either an S -, P - or D -wave state. One assumes that the third pion, being fast in the B -meson decay frame, does not interact with this pair. This hypothesis is mainly valid in a limited range of the $\pi^+\pi^-$ effective mass, here taken between the $\pi\pi$ threshold and 1.64 GeV.

The short-distance interaction part of the decay amplitudes describes the flavor changing processes $b \rightarrow u\bar{u}d$ and $b \rightarrow d\bar{d}d$. It is proportional to Cabibbo-Kobayashi-Maskawa matrix elements multiplied by effective coefficients calculable in the perturbative QCD formalism. This short-distance amplitude is multiplied by a long-distance contribution expressed in terms of two products. The first one is the product of the pion decay constant by the $B \rightarrow \pi\pi$ transition matrix element and the second one is the product of the pion form factor by the $B \rightarrow \pi$ transition form factor. The parametrization [Eqs. (18), (19)] of the scalar and vector B to π transition form factors follow from the light-cone sum rule study of Ref. [21].

The effective Wilson coefficients are calculated to next-to-leading order in the strong coupling constant. They include vertex and penguin corrections but neither hard-scattering ones nor annihilation contributions since these last two terms contain unknown phenomenological parameters related to amplitude divergences [9]. We find that these vertex and penguin corrections are small in comparison to the leading order term (see Table 1). However, they allow to generate some non-zero CP asymmetries.

We then assume the B to $\pi\pi$ transition matrix element to be equal to the product of the B to intermediate meson transition form factor by the

decay amplitude of this meson into two pions being either in S , P or D wave. The next step is to suppose the latter decay amplitude to be proportional to the pion non-strange scalar or vector form factor depending on the wave studied. For the S wave the proportionality factor is given by a fitted parameter χ_S and for the P wave it is related to the inverse of the ρ decay constant. For the limited range of the effective $\pi\pi$ mass, from $\pi\pi$ threshold to 1.64 GeV, the $B \rightarrow \pi\pi$ transition form factors are taken as constants given by the $B \rightarrow f_0(980)$ [19] and by the $B \rightarrow \rho(770)$ [20] transition form factors at $q^2 = m_\pi^2$. The decay amplitude for the $\pi\pi$ D wave is described by a relativistic Breit-Wigner formula and the not well known B to $f_2(1270)$ transition form factor is fitted. We find $F^{Bf_2}(m_\pi^2) = 0.098 \pm 0.007$.

The pion scalar form factor is modeled by the unitary relativistic three coupled-channel equation (27) using the $\pi\pi$, $K\bar{K}$ and effective $(2\pi)(2\pi)$ scattering T matrix of Refs. [29, 30]. This form factor depends on two fitted parameters: the first one κ insures the convergence of the involved integrals and the second one, c , controls the high-energy behavior of the production functions accountable for the meson pair formation. The pion vector form factor takes into account the contribution of the $\rho(770)$, $\rho(1450)$ and $\rho(1700)$, and follows from the parametrization of the Belle Collaboration in their study of the semi-leptonic $\tau^- \rightarrow \pi^- \pi^0 \nu_\tau$ decays. For the P -wave amplitude we introduce a fitted correction factor N_P .

We obtain a good fit to the $\pi\pi$ effective mass distributions of the BABAR Collaboration data of the $B^\pm \rightarrow \pi^\pm \pi^\mp \pi^\pm$ decays [5]. The value of the branching fraction for the $B^\pm \rightarrow \rho(770)^0 \pi^\pm$ decays, $(8.1 \pm 0.7 \pm 1.2_{-1.1}^{+0.4}) \times 10^{-6}$, is well reproduced with the correction factor N_P close to 1. This shows that the QCD factorization gives the right strength of the B to $\rho\pi$ decay amplitude. The $\pi^+\pi^-$ spectra are dominated by the $\rho(770)^0$ resonance but, at low effective mass, the S -wave contribution is sizable. Here the $f_0(600)$ resonance manifests its presence. Furthermore one observes a strong interference of the S and P waves in the event distributions for $\cos\theta > 0$ and $\cos\theta < 0$. Here the $f_0(980)$ is not directly visible as a peak, since the pion scalar form factor has a dip near 1 GeV. The surplus of events in the $\pi^+\pi^-$ effective mass close to 1.25 GeV is well described by the contribution of the $f_2(1270)$ resonance. The branching fraction for $B^\pm \rightarrow f_2(1270)\pi^\pm$, $f_2(1270) \rightarrow \pi^+\pi^-$ decay is found to be of $(2.8 \pm 0.4) \times 10^{-6}$. At 1.4 GeV, the tiny maximum of the S -wave distribution comes from the scalar resonance $f_0(1400)$ [29, 30].

Our model yields a unified description of the contribution of the three scalar resonances $f_0(600)$, $f_0(980)$ and $f_0(1400)$ in terms of one function: the pion non-strange scalar form factor. This reduces strongly the number of needed free parameters to analyze the Dalitz plot. The functional form of our S -wave amplitude [Eq. (22)], proportional to $\Gamma_1^{n*}(s)$, could be used in Dalitz-plot analyses and the table of $\Gamma_1^{n*}(s)$ values can be sent upon request.

The strong interaction phases of the decay amplitudes are constrained by unitarity and meson-meson data. Their determination should help in the extraction of the weak angle phase γ or ϕ_3 equal to $\arg(-\lambda_u^*/\lambda_c^*)$. Of course new experimental data with better statistics would be welcome. One expects $B^\pm \rightarrow \pi^\pm \pi^\mp \pi^\pm$ events from the Belle Collaboration, and probably, in the near future, from LHCb and from the near term super B factories.

The authors are obliged to Bachir Moussallam for providing them the values of his pion scalar form factor $\Gamma_1^n(s)$ and to Gagan Bihari Mohanty for useful comments on the BABAR data. We are very grateful to Maria Rózańska, Bachir Moussallam, Eli Ben-Haim and José Ocariz for helpful discussions. This work has been supported in part by the Polish Ministry of Science and Higher Education (grant No N N202 248135) and by the IN2P3-Polish Laboratories Convention (project No 08-127).

Appendix A

Long-distance functions $X_{S,P,D}$ and $Y_{S,P}$

Appendix A.1 The function X_S from the S -wave amplitude proportional to BR_S transition matrix element

From Eq. (13) the function X_S reads

$$\begin{aligned} X_S &\equiv \langle [\pi^+(p_2)\pi^-(p_3)]_S | (\bar{u}b)_{V-A} | B^- \rangle \langle \pi^- | (\bar{d}u)_{V-A} | 0 \rangle \\ &= G_{R_S \pi^+ \pi^-}^n(s_{23}) \langle R_S | (\bar{u}b)_{V-A} | B^- \rangle \langle \pi^- | (\bar{d}u)_{V-A} | 0 \rangle, \end{aligned} \quad (\text{A.1})$$

where the vertex function $G_{R_S \pi^+ \pi^-}^n(s_{23})$ describes the R_S decay into a $[\pi^+ \pi^-]_S$ pair. The B to R_S transition matrix element reads (see e.g. Eq. (B6) of Ref. [12])

$$\begin{aligned} \langle R_S(p_2 + p_3) | \bar{u} \gamma^\mu (1 - \gamma^5) b | B^-(p_B) \rangle = \\ i \left\{ \left[(p_B + p_2 + p_3)^\mu - \frac{M_B^2 - s_{23}}{m_\pi^2} p_1^\mu \right] F_1^{BR_S}(m_\pi^2) + \frac{M_B^2 - s_{23}}{m_\pi^2} p_1^\mu F_0^{BR_S}(m_\pi^2) \right\}, \end{aligned} \quad (\text{A.2})$$

where $F_0^{BR_S}(m_\pi^2)$ and $F_1^{BR_S}(m_\pi^2)$ are the BR_S scalar and vector form factors, respectively. The pion decay constant f_π is defined as

$$\langle \pi^-(p_1) | \bar{d} \gamma_\mu (1 - \gamma_5) u | 0 \rangle = i f_\pi p_{1\mu}. \quad (\text{A.3})$$

The product of Eqs. (A.2) and (A.3) yields

$$\langle R_S | (\bar{u}b)_{V-A} | B^- \rangle \langle \pi^- | (\bar{d}u)_{V-A} | 0 \rangle = -(M_B^2 - s_{23}) f_\pi F_0^{BR_S}(m_\pi^2). \quad (\text{A.4})$$

The vertex function $G_{R_S \pi^+ \pi^-}^n(s_{23})$, as in Ref. [2], is modeled by

$$\langle [\pi^+ \pi^-]_S | \bar{n}n | 0 \rangle = G_{R_S \pi^+ \pi^-}^n(s_{23}) \langle R_S | \bar{n}n | 0 \rangle. \quad (\text{A.5})$$

An effective scalar decay constant $f_{R_S}^n$ can be introduced with

$$\langle R_S | \bar{n}n | 0 \rangle = m_{R_S} f_{R_S}^n. \quad (\text{A.6})$$

From Eqs. (A.5), (20) and (A.6) one obtains

$$G_{R_S \pi^+ \pi^-}^n(s_{23}) = \sqrt{\frac{2}{3}} \chi_S \Gamma_1^{n*}(s_{23}) = \sqrt{\frac{2}{3}} \frac{\sqrt{2} B_0}{m_{R_S} f_{R_S}^n} \Gamma_1^{n*}(s_{23}), \quad (\text{A.7})$$

with

$$\chi_S = \frac{\sqrt{2} B_0}{m_{R_S} f_{R_S}^n}. \quad (\text{A.8})$$

The effective scalar decay constant has a role comparable to the R_P decay constant as can be seen comparing Eqs. (A.7) and (A.19). The product of Eqs. (A.7), (A.2) and (A.3) gives

$$X_S = -\sqrt{\frac{2}{3}} \chi_S f_\pi (M_B^2 - s_{23}) F_0^{BR_S}(m_\pi^2) \Gamma_1^{n*}(s_{23}). \quad (\text{A.9})$$

Appendix A.2 The function Y_S from the S -wave amplitude proportional to $B\pi$ transition matrix element

From Eq. (14) one has

$$\begin{aligned} Y_S &\equiv \langle \pi^- | (\bar{d}b)_{sc-ps} | B^- \rangle \langle [\pi^+(p_2) \pi^-(p_3)]_S | (\bar{d}d)_{sc+ps} | 0 \rangle \\ &= \langle \pi^- | \bar{d}b | B^- \rangle \langle [\pi^+(p_2) \pi^-(p_3)]_S | \bar{d}d | 0 \rangle. \end{aligned} \quad (\text{A.10})$$

From the Dirac equations satisfied by $b(p_B)$ and $\bar{d}(p_1)$ one obtains

$$\langle \pi^-(p_1) | \bar{d}(p_1) b(p_B) | B^-(p_B) \rangle = \left\langle \pi^-(p_1) \left| \bar{d}(p_1) \frac{\gamma \cdot (p_B - p_1)}{m_b - m_d} b(p_B) \right| B^-(p_B) \right\rangle. \quad (\text{A.11})$$

The B to π transition matrix element $\langle \pi^- | (\bar{d}b)_{V-A} | B^- \rangle$, entering into the above expression, can be written as (see e.g. Eq. (5) of Ref. [3])

$$\begin{aligned} & \langle \pi^-(p_1) | \bar{d} \gamma^\mu (1 - \gamma^5) b | B^-(p_B) \rangle \\ &= \left[(p_B + p_1)^\mu - \frac{M_B^2 - m_\pi^2}{q^2} q^\mu \right] F_1^{B\pi}(q^2) + \frac{M_B^2 - m_\pi^2}{q^2} q^\mu F_0^{B\pi}(q^2), \end{aligned} \quad (\text{A.12})$$

where $F_0^{B\pi}(q^2)$ and $F_1^{B\pi}(q^2)$ are the $B\pi$ scalar and vector form factors, respectively and $q = p_B - p_1 = p_2 + p_3$. Using Eqs. (A.12) and (20) in Eq. (A.10), yields

$$Y_S = \sqrt{\frac{2}{3}} B_0 \Gamma_1^{n*}(s_{23}) \frac{M_B^2 - m_\pi^2}{m_b - m_d} F_0^{B\pi}(s_{23}). \quad (\text{A.13})$$

Appendix A.3 The function X_P from the P -wave amplitude proportional to BR_P transition matrix element

From Eq. (15) one has for the function X_P (see Eq. (3.1) of Ref. [12])

$$\begin{aligned} X_P &\equiv \langle [\pi^+(p_2)\pi^-(p_3)]_P | (\bar{u}b)_{V-A} | B^- \rangle \langle \pi^- | (\bar{d}u)_{V-A} | 0 \rangle \\ &= \frac{G_{R_P\pi^+\pi^-}^n(s_{23})}{\sqrt{2}} \epsilon \cdot (p_2 - p_3) \langle R_P | (\bar{u}b)_{V-A} | B^- \rangle \langle \pi^- | (\bar{d}u)_{V-A} | 0 \rangle \end{aligned} \quad (\text{A.14})$$

where the R_P decay into a $[\pi^+\pi^-]_P$ pair is described by the vertex function $G_{R_P\pi^+\pi^-}^n(s_{23})$. Here ϵ represents the polarization vector of the P -wave meson R_P . The factor $1/\sqrt{2}$ comes from the fact that R_P represents the $\rho(770)^0$. As seen from e.g. Eq. (B6) of Ref. [12] or Eq. (24) of Ref. [6],

$$\begin{aligned} \langle R_P(p_2 + p_3) | (\bar{u}b)_{V-A} | B^-(p_B) \rangle &= -i 2m_{R_P} \frac{\epsilon^* \cdot p_B}{p_1^2} p_1 A_0^{BR_P}(p_1^2) \\ &\quad + \text{other terms.} \end{aligned} \quad (\text{A.15})$$

The ‘‘other terms’’ do not give any contribution when multiplying this matrix element by that given in Eq. (A.3). Plugging this expression into Eq. (A.14) one has a product of polarization vectors and the sum over the three possible polarization eigenvalues of the state R_P should be done. From

$$\sum_{\lambda=0,\pm 1} \epsilon_\mu^\lambda(p) \epsilon_\nu^{\lambda*}(p) = -(g_{\mu\nu} - \frac{p_\mu p_\nu}{p^2}), \quad (\text{A.16})$$

one obtains

$$\sum_{\lambda=0,\pm 1} \epsilon^\lambda \cdot (p_2 - p_3) \epsilon^{\lambda*} \cdot p_B = -p_1 \cdot (p_2 - p_3). \quad (\text{A.17})$$

Then

$$X_P = N_P \frac{f_\pi}{f_{R_P}} (s_{13} - s_{12}) A_0^{BR_P}(m_\pi^2) F_1^{\pi\pi}(s_{23}). \quad (\text{A.18})$$

Above, as shown in Ref. [3] for the $K^*(892) \rightarrow (K\pi)_P$ decay case [see their Eq. (D9)], we have parametrized the $R_P\pi^+\pi^-$ vertex function in terms of the pion vector form factor $F_1^{\pi\pi}(s_{23})$. One has

$$G_{R_P\pi^+\pi^-}(s_{23}) = N_P \frac{\sqrt{2}}{m_{R_P} f_{R_P}} F_1^{\pi\pi}(s_{23}), \quad (\text{A.19})$$

f_{R_P} being the charged R_P decay constant. Above we have introduced a parameter N_P to take into account the possible deviation of the strength of the P wave, here proportional to $1/f_{R_P}$.

Appendix A.4 **The function Y_P from the P -wave amplitude proportional to the $B\pi$ transition matrix element**

From Eq. (16)

$$Y_P \equiv \langle \pi^- | (\bar{d}b)_{V-A} | B^- \rangle \langle [\pi^+(p_2)\pi^-(p_3)]_P | (\bar{u}u)_{V-A} | 0 \rangle. \quad (\text{A.20})$$

The pion vector form factor is defined by (see e.g. Eq. (36) of Ref. [6])

$$\langle R_P | (\bar{u}u)_{V-A} | 0 \rangle = \langle [\pi^+(p_2)\pi^-(p_3)]_P | \bar{u}\gamma_\mu(1-\gamma_5)u | 0 \rangle = -(p_2 - p_3)_\mu F_1^{\pi\pi}(q^2). \quad (\text{A.21})$$

The minus sign arises from the definition of the form factor $F_1^{\pi\pi}(q^2)$ which contains a plus sign for a $(\bar{d}d)_{V-A}$ current [similar to Eq. (A.12)], then as $\rho^0 = 1/\sqrt{2}(u\bar{u} - d\bar{d})$, there will be a minus sign for a $(\bar{u}u)_{V-A}$ current. The product of Eqs. (A.12) and (A.21) gives

$$Y_P = -2 p_1 \cdot (p_2 - p_3) F_1^{B\pi}(q^2) F_1^{\pi\pi}(q^2) = (s_{13} - s_{12}) F_1^{B\pi}(q^2) F_1^{\pi\pi}(q^2). \quad (\text{A.22})$$

Appendix A.5 **The function X_D from the D -wave amplitude proportional to BR_D transition matrix element**

From Eq. (17) one has

$$\begin{aligned}
X_D &\equiv \langle [\pi^+(p_2)\pi^-(p_3)]_D | (\bar{u}b)_{V-A} | B^- \rangle \langle \pi^-(p_1) | (\bar{d}u)_{V-A} | 0 \rangle \\
&= \frac{1}{\sqrt{2}} G_{R_D \pi^+ \pi^-}(s_{23}) \sum_{\lambda=-2}^2 \epsilon_{\alpha\beta} p_2^\alpha p_3^\beta \langle R_D^\lambda(p_D) | (\bar{u}b)_{V-A} | B^- \rangle \\
&\qquad\qquad\qquad \langle \pi^-(p_1) | (\bar{d}u)_{V-A} | 0 \rangle, \quad (\text{A.23})
\end{aligned}$$

with $p_D = p_2 + p_3$. The factor of $1/\sqrt{2}$ is due to the quark content of the resonance R_D [the meson $f_2(1270)$]. The R_D decay into a $[\pi^+\pi^-]_D$ pair is described by the vertex function $G_{R_D \pi^+ \pi^-}(s_{23})$. Here $\epsilon_{\alpha\beta}(\lambda)$ represents the polarization tensor of the $f_2(1270)$ and λ is its spin projection (see Ref. [38], p. 147). Taking Eq. (A3) for $\langle \pi^-(p_1) | (\bar{d}u)_{V-A} | 0 \rangle$ and Eq. (4) of Ref. [23] for the transition matrix element $\langle R_D^\lambda(p_D) | (\bar{u}b)_{V-A} | B^- \rangle$ we obtain

$$X_D = -\frac{f_\pi}{\sqrt{2}} G_{R_D \pi^+ \pi^-}(s_{23}) F^{BR_D}(m_\pi^2) \sum_{\lambda=-2}^2 \epsilon_{\alpha\beta}(\lambda) p_2^\alpha p_3^\beta \epsilon_{\mu\nu}^*(\lambda) p_B^\nu p_1^\mu. \quad (\text{A.24})$$

To be consistent with the choice of normalization of Eq. (A2), we have multiplied by i the right hand side of Eq. (4) in Ref. [23]. One can show that (see Eqs. (7.7) and (7.8) of Ref. [38], p. 73)

$$D(s_{12}, s_{23}) \equiv \sum_{\lambda=-2}^2 \epsilon_{\alpha\beta}(\lambda) p_2^\alpha p_3^\beta \epsilon_{\mu\nu}^*(\lambda) p_B^\nu p_1^\mu = \frac{1}{3} (|\vec{p}_1||\vec{p}_2|)^2 - (\vec{p}_1 \cdot \vec{p}_2)^2, \quad (\text{A.25})$$

\vec{p}_1 and \vec{p}_2 being the momenta of the $\pi^-(p_1)$ and the $\pi^+(p_2)$ in the rest frame of $\pi^+(p_2)$ and $\pi^-(p_3)$. One obtains , with $m_{23} = \sqrt{s_{23}}$,

$$\begin{aligned}
\vec{p}_1 \cdot \vec{p}_2 &= \frac{1}{4}(s_{13} - s_{12}), \\
|\vec{p}_2| &= \frac{1}{2} \sqrt{m_{23}^2 - 4m_\pi^2}, \quad |\vec{p}_2| = |\vec{p}_3|, \\
|\vec{p}_1| &= \frac{1}{2m_{23}} \sqrt{\left[M_B^2 - (m_{23} + m_\pi)^2 \right] \left[M_B^2 - (m_{23} - m_\pi)^2 \right]}, \quad (\text{A.26})
\end{aligned}$$

which allows to express Eq. (A.25) in terms of s_{12} and s_{23} . The vertex function entering into Eq. (A.23) is parametrized as being proportional to a relativistic Breit-Wigner resonance formula, we write

$$G_{R_D\pi^+\pi^-}(s_{23}) = \sqrt{\frac{2}{3}} \frac{G_{f_2}}{m_{R_D}^2 - s_{23} - im_{R_D}\Gamma(s_{23})}, \quad (\text{A.27})$$

where (see Ref. [38], p.147)

$$G_{f_2} = m_{f_2} \sqrt{\frac{60\pi\Gamma_{f_2\pi\pi}}{q_{f_2}^5}}, \quad \Gamma_{f_2\pi\pi} = 0.848 \Gamma_{f_2} \quad (\text{A.28})$$

and the mass-dependent width $\Gamma(s_{23})$ can be expressed as (see Eq. (7) of Ref. [5]),

$$\Gamma(s_{23}) = \Gamma_{f_2} \left(\frac{|\vec{p}_2|}{q_{f_2}} \right)^5 \frac{m_{f_2} X(|\vec{p}_2|)}{m_{23} X(q_{f_2})}. \quad (\text{A.29})$$

Here Γ_{f_2} is the total width of the $f_2(1270)$ resonance, m_{f_2} its mass and q_{f_2} is the pion momentum in the f_2 c.m. system. The Blatt-Weisskopf barrier form factor is given by [5]

$$X(z) = \frac{1}{(zr_{BW})^4 + 3(zr_{BW})^2 + 9}, \quad (\text{A.30})$$

where the meson radius parameter $r_{BW} = 4 \text{ (GeV/c)}^{-1}$. Finally one has

$$X_D = -\frac{1}{\sqrt{2}} f_\pi F^{BR_D}(m_\pi^2) \sqrt{\frac{2}{3}} \frac{G_{f_2} D(s_{12}, s_{23})}{m_{R_D}^2 - s_{23} - im_{R_D}\Gamma(s_{23})}. \quad (\text{A.31})$$

Appendix B

Linear system of equations for α_i^n , τ_i^n and ω_i^n

The linear system of nine equations satisfied by the nine production function parameters α_i^n , τ_i^n and ω_i^n , $i = 1, 2, 3$, is

$$\begin{aligned} \alpha_i^n + \sum_{j=1}^3 \alpha_j^n H_{ji}(0) &= d_i^n, \\ \tau_i^n + \sum_{j=1}^3 \left(\tau_j^n H_{ji}(0) + \alpha_j^n \frac{\partial H_{ji}(E)}{\partial E} \Big|_{E=0} \right) &= 0, \\ \omega_i^n + \sum_{j=1}^3 \left(\omega_j^n H_{ji}(0) + \tau_j^n \frac{\partial H_{ji}(E)}{\partial E} \Big|_{E=0} + \frac{1}{2} \alpha_j^n \frac{\partial^2 H_{ji}(E)}{\partial E^2} \Big|_{E=0} \right) &= f_i^n. \end{aligned} \quad (\text{B.1})$$

REFERENCES

- [1] A. Furman, R. Kamiński, L. Leśniak and B. Loiseau, Phys. Lett. B **622**, 207 (2005), *Long-distance effects and final state interactions in $B \rightarrow \pi\pi K$ and $B \rightarrow K\bar{K}K$ decays.*
- [2] B. El-Bennich, A. Furman, R. Kamiński, L. Leśniak and B. Loiseau, Phys. Rev. D **74**, 114009 (2006), *Interference between $f_0(980)$ and $\rho(770)^0$ resonances in $B \rightarrow \pi^+\pi^-K$ decays.*
- [3] B. El-Bennich, A. Furman, R. Kamiński, L. Leśniak, B. Loiseau, B. Moussallam, Phys. Rev. D **79**, 094005 (2009), *CP violation and kaon-pion interactions in $B \rightarrow K\pi^+\pi^-$ decays.*
- [4] O. Leitner, J.-P. Dedonder, B. Loiseau, and R. Kamiński, Phys. Rev. D **81**, 094033 (2010), *K^* resonance effects on direct CP violation in $B \rightarrow \pi\pi K$.*
- [5] B. Aubert, et al. (BABAR Collaboration), Phys. Rev. D **79**, 072006 (2009), *Dalitz-plot analysis of $B^\pm \rightarrow \pi^\pm\pi^\mp\pi^\pm$ decays.*
- [6] A. Ali, G. Kramer and Cai-Dian Lü, Phys. Rev. D **58**, 094009 (1998), *Experimental tests of factorization in charmless nonleptonic two-body B decays.*
- [7] M. Beneke, G. Buchalla, M. Neubert and C. T. Sachrajda, Nucl. Phys. **B606**, 245 (2001), *QCD factorization in $B \rightarrow \pi K, \pi\pi$ decays and extraction of Wolfenstein parameters.*
- [8] S. Gardner and U.-G. Meißner, Phys. Rev. D **65**, 094004 (2002), *Rescattering and chiral dynamics in $B \rightarrow \rho\pi$ decays.*
- [9] M. Beneke and M. Neubert, Nucl. Phys. **B675**, 333 (2003), *QCD factorization for $B \rightarrow PP$ and $B \rightarrow PV$ decays.*
- [10] O. Leitner, X-H. Guo, A.W. Thomas, J. Phys. G: Nucl. Part. Phys. **31**, 199 (2005), *Direct CP violation, branching ratios and form factors $B \rightarrow \pi$, $B \rightarrow K$ in B decays.*
- [11] H. Y. Cheng, C. K. Chua and K. C. Yang, Phys. Rev. D **73**, 014017 (2006), *Charmless hadronic B decays involving scalar mesons: implications to the nature of light scalar mesons.*
- [12] H-Y. Cheng, C-K. Chua and A. Soni, Phys. Rev D **76**, 094006 (2007), *Charmless three-body decays of B mesons.*
- [13] M. Beneke, Nucl. Phys. B (Proc. Suppl.) **170**, 57 (2007), *Hadronic B decays.*
- [14] A. Deandrea and A. D. Polosa, Phys. Rev. Lett. **86**, 216 (2001), *$B \rightarrow \rho\pi$ decays, Resonant and Nonresonant Contributions.*
- [15] B. Aubert, et al. (BABAR Collaboration), Phys. Rev. D **76**, 012004 (2007), *Measurement of CP-violating asymmetries in $B^0 \rightarrow (\rho\pi)^0$ using a time-dependent Dalitz-plot analysis.*
- [16] A. Kusaka, et al. (Belle Collaboration), Phys. Rev. D **77**, 072001 (2008), *Measurement of CP asymmetries and branching fractions in a time-dependent Dalitz-plot analysis of $B^0 \rightarrow (\rho\pi)^0$ and a constraint on the quark mixing angle ϕ_2 .*

- [17] M. Beneke in Three-Body Charmless B Decays Workshop, <http://lphne-babar.in2p3.fr/3BodyCharmlessWS/>, February 1-3, 2006, LPNHE, Paris, *Quasi two-body and three-body decays in the heavy quark expansion*.
- [18] K. Nakamura *et al.* (Particle Data Group), J. Phys. G **37** 075021 (2010), *Review of particle physics*.
- [19] B. El-Bennich, O. Leitner, J.-P. Dedonder, B. Loiseau, Phys. Rev. D **79**, 076004 (2009), *The Scalar Meson $f_0(980)$ in Heavy-Meson Decays*.
- [20] P. Ball, V. M. Braun, Phys. Rev. D **58**, 094016 (1998), *Exclusive semileptonic and rare B meson decays in QCD*.
- [21] P. Ball and R. Zwicky Phys. Rev. D **71**, 014015 (2005), *New results on $B \rightarrow \pi, K, \eta$ decay form factors from light-cone sum rules*.
- [22] U.-G. Meißner and J. A. Oller, Nucl. Phys. **A679**, 671 (2001), *$J/\psi \rightarrow \phi\pi\pi(K\bar{K})$ decays, chiral dynamics and OZI violation*.
- [23] C. S. Kim, Jong-Phil Lee, and Sechul Oh, Phys. Rev. D **67**, 014002 (2003) [8 pages] *Nonleptonic two-body charmless B decays involving a tensor meson in the ISGW2 model*.
- [24] G. Barton, *Introduction to dispersion techniques in field theory*, Benjamin, New-York, 1965.
- [25] H.-Y. Cheng, C. K. Chua and C. W. Hwang, Phys Rev. D **69**, 074025 (2004), *Covariant light-front approach for S-wave and P-wave mesons: Its application to decay constants and form factors*.
- [26] N. I. Muskhelishvili, Singular integral equations, (P.Nordhof 1953), chapters 18 and 19; R. Omnès, Nuovo Cim. **8**, 316 (1958), *On the Solution of certain singular integral equations of quantum field theory*.
- [27] J. F. Donoghue, J. Gasser, H. Leutwyler, Nucl. Phys. **343**, 341 (1990), *The decay of a light Higgs boson*.
- [28] B. Moussallam, Eur. Phys. J. C **14**, 111 (2000), *N_f dependence of the quark condensate from a chiral sum rule*.
- [29] R. Kamiński, L. Leśniak and B. Loiseau, Phys. Lett. B **413** (1997) 130, *Three channel model of meson meson scattering and scalar meson spectroscopy*.
- [30] R. Kamiński, L. Leśniak and B. Loiseau, Eur. Phys. J. **C9**, 141 (1999), *Scalar mesons and multichannel amplitudes*.
- [31] R. Kamiński and L. Leśniak, J.-P. Maillet, Phys. Rev. D **50**, 3145 (1994), *Relativistic effects in scalar meson dynamics*.
- [32] Yoshio Yamaguchi and Yoriko Yamaguchi, Phys. Rev. **95**, 1635 (1954), *Two-Nucleon Problem When the Potential Is Nonlocal but Separable. II*.
- [33] T. A. Lähde, and U.-G. Meißner, Phys. Rev. D **74**, 034021 (2006), *Improved analysis of J/ψ decays into a vector meson and two pseudoscalars*.
- [34] C. Allton, *et al.* (RBC and UKQCD Collaborations), Phys. Rev. D **78**, 114509 (2008), *Physical results from 2 + 1 flavor domain wall QCD and $SU(2)$ chiral perturbation theory*.

- [35] M. Fujikawa *et al.* (Belle Collaboration), Phys. Rev. D **78**, 072006 (2008), *High-statistics study of the $\tau^- \rightarrow \pi^- \pi^0 \nu_\tau$ decay.*
- [36] P. Ball and G. W. Jones, JHEP 0703, 69 (2007), *Twist-3 distribution amplitudes of K^* and ϕ mesons.*
- [37] B. Moussallam, private communication.
- [38] H. Pilkuhn, *The interactions of hadrons*, North-Holland P. C., 1967.